Modeling and Control of Co-Surge in Bi-Turbo Engines

Andreas Thomasson and Lars Eriksson

Linköping University Post Print

N.B.: When citing this work, cite the original article.

Original Publication:

Andreas Thomasson and Lars Eriksson, Modeling and Control of Co-Surge in Bi-Turbo Engines, 2011, Proceedings of the 18th IFAC World Congress, 2011, 13010-13015.
http://dx.doi.org/10.3182/20110828-6-IT-1002.02338

2011 IFAC World Congress, Milano, Milano, Italy, 28 August - 2 September

Copyright: International Federation of Automatic Control (IFAC)
http://www.ifac-control.org/

Postprint available at: Linköping University Electronic Press
http://urn.kb.se/resolve?urn=urn:nbn:se:liu:diva-70390

Modeling and Control of Co-Surge in Bi-Turbo Engines ⋆

Andreas Thomasson * **Lars Eriksson** *

* *Vehicular Systems, Dept. of Electrical Engineering Linköping University, SE-581 83 Linköping, Sweden, {andreast,larer}@isy.liu.se*

Abstract:
Using a bi-turbocharged configuration makes for better utilization of the exhaust energy and a faster torque response in V-type engines. A special surge phenomenon that should be avoided in bi-turbocharged engines is co-surge, which is when the two interconnected compressors alternately go into flow reversals. If co-surge should occur, the control system must be able to quell the oscillations with as little disturbance in torque as possible. This paper presents a model of a bi-turbocharged engine based on a Mean Value Engine Model that includes a More-Greizer compressor model for surge. The model is validated against measured data showing that it captures the frequency and amplitude of the co-surge oscillation. The effect of momentum conservation in the pipes is investigated by adding this feature to the control volumes before and after the compressor. This gives a slightly better mass flow shape with the drawback of increased simulation time, due to more states and a higher frequency content in the model. A sensitivity analysis is performed to investigate which model parameters have most influence on the co-surge behavior. It is shown that the largest influence comes from the turbocharger inertia, the volumes after the compressor and the "zero mass flow pressure ratio" during flow reversal in the compressor. The model is used to investigate principles for control strategies to detect and quell co-surge. The detection algorithm is evaluated on measured data.

Keywords: Compressor surge, parameter sensitivity, surge detection, surge control

1. INTRODUCTION

More advanced turbocharging concepts are constantly being developed to increase power density, and to reduce fuel consumption and emissions of internal combustion engines. For V-type engines one option is to use two smaller parallel turbos and let the exhausts from the two cylinder banks feed separate turbines. In this way the turbines can be placed closer to the exhaust ports than with a single larger turbo. Heat losses are reduced which increases the available energy to the turbochargers. With fewer cylinders feeding each turbine it is also possible to make better use of the pulsating flow, increasing the energy extracted from the exhaust.

In a bi-turbocharged engine the two air paths are connected before the throttle. If a disturbance alters the mass flow balance between them, when operating close to the surge line on an otherwise stable operating point, one compressor can be pushed into the surge region and the mass flow reverses. When the compressor recovers it can push the other compressor into surge, starting an oscillation where the mass flow through the compressors alternately reverses. Compressor surge should be avoided and considered when developing the control system for a bi-turbocharged engine.

⋆ This research was supported by the Linnaeus Center CADICS, funded by the Swedish Research Council.

1.1 Contributions and Outline

Compressor surge has been extensively studied during the 70's and 80's and a well known modeling result is the More-Greitzer model (Greitzer, 1981). The majority of the work has been on turbo machinery with gas turbines. A survey of surge modeling and control is given in Willems and de Jager (1998) and there is also a substantial treatment in Gravdahl (1998). For automotive turbochargers there are only a few studies on surge where most utilize the More-Greitzer model, see e.g. Ammann et al. (2001) or Leufven and Eriksson (2008). The main contribution of this paper is the analysis of experimental data and modeling of co-surge. In addition a method for co-surge detection and a co-surge controller are proposed.

Experimental data on co-surge and an analysis of the phenomenon is presented in section 2. In sections 3 and 4 a model for the bi-turbocharged engine, based on a Mean Value Engine Model (MVEM) structure, and surge capable compressor model is presented. The model's capability to capture co-surge is verified in section 5 and a parameter sensitivity analysis is presented. Section 6 investigates the effects of extending the model with pipes that conserve momentum. An algorithm for detecting co-surge and a control strategy for restoring the mass flow balance is presented. The detection algorithm is validated against measured data and the control strategy is evaluated on the model in section 7, followed by conclusions in section 8.

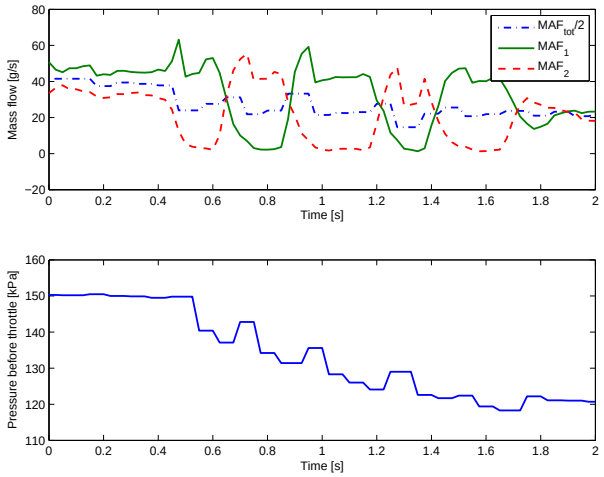

Fig. 1. *Top:* An example of co-surge measured on a test vehicle. The green solid line and red dashed line are measured mass flows in the respective air path. The blue dash dotted line is half the total mass flow. The oscillation frequency is approximately 1.9 Hz. It should be mentioned that the mass flow sensors can not measure negative mass flow, and saturate at 0 g/s. *Bottom:* Corresponding boost pressure. The pressure is dropping with peaks of 7 kPa shortly after the mass flows switch.

2. CO-SURGE

An example of co-surge measured in a test vehicle is shown in figure 1. The three mass flow sensors are placed approximately 50 cm after the air filter, 80 cm before the compressors, one directly before and two directly after the air path is divided. The mass flow sensors are of hot film type, MAF_1 and MAF_2 are sampled at 40 Hz while MAF_{tot} is sampled at 12.5 Hz. The mass flow balance between the two air paths is slightly unbalanced. After a small decrease in mass flow, one compressor flow reverses, starting an oscillation between the compressors. Surge occurs when the pressure ratio is too high so that the mass flow can not be maintained. When the compressor enters this region the mass flow will start to reverse. The flow is not recovered until the pressure ratio has decreased sufficiently. Co-surge is a condition in the bi-turbo configuration, where the mass flow through the compressors alternately reverses. When one compressor enters surge more air will flow through the other compressor due to the pressure ratio decrease. As the first compressor recovers the second compressor is pushed into surge. Compared to normal surge, co-surge has a much lower frequency, roughly one order of magnitude. This indicates that co-surge is more than standard compressor surge with alternating flow reversals.

3. ENGINE MODEL

To investigate the effect of different engine components on co-surge, a physical model of the system is of use. Depending on the accuracy of the model it can give quantitative or qualitative results on the effect of different configurations and parameters. The model can also be used to test and evaluate different control strategies before trying them in the real environment.

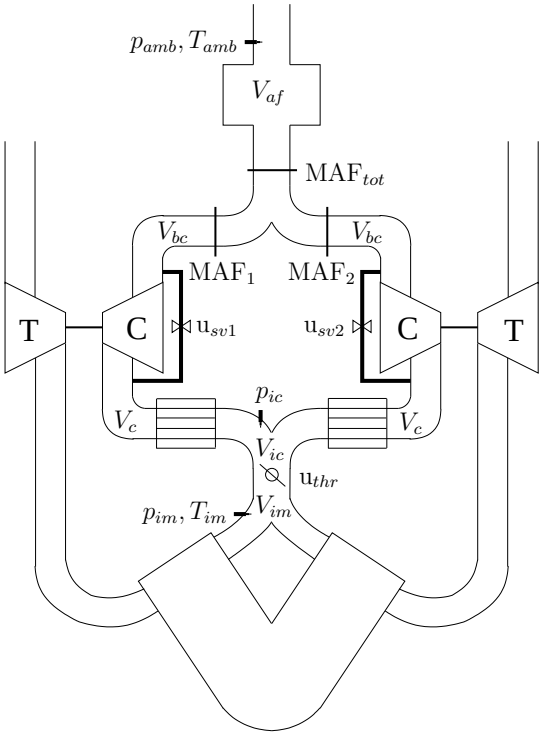

Fig. 2. A sketch of the bi-turbocharged engine configuration studied in this paper. A mass flow sensor is positioned after the common air filter and two more directly after the two air paths split up. The actuators used in the control section are the two surge valves, u_{sv1}, u_{sv2}, and the throttle, u_{thr}.

The modeling approach taken is the component based Mean Value Engine Model (MVEM) outlined in Eriksson et al. (2002); Eriksson (2007). This uses control volumes, that contain states for pressure and temperature, and restrictions that govern the mass flow. A complete turbocharged spark ignited engine with these components is implemented and evaluated in Andersson (2005). For this investigation the MVEM components have been arranged in a bi-turbo structure to resemble the engine in figure 2. Two banks contain all doubled components, compressor, one cylinder bank, turbine and exhaust system. In the middle are the common parts for the two air paths, air filter, throttle and intake manifold.

The two turbo shafts are modeled by Newtons second law of motion, utilizing the power balance between compressor and turbine and a viscous friction term:

$$J_{tc}\frac{\omega_{tc}}{dt} = \frac{P_t}{\omega_{tc}} - \frac{P_c}{\omega_{tc}} - k_{fric}\omega_{tc} \tag{1}$$

The compressor power consumption is derived from the first law of thermodynamics and given by the equation:

$$P_c = W_c c_p (T_{out} - T_{in}) \tag{2}$$

The expression for the turbine is similar, see Eriksson (2007) for the turbine model. Next section presents the surge capable compressor.

4. COMPRESSOR MODEL

To model surge the compressor model must handle the reverse mass flow. This is achieved by the well known and well tested More-Greizer model (Greitzer, 1981), that

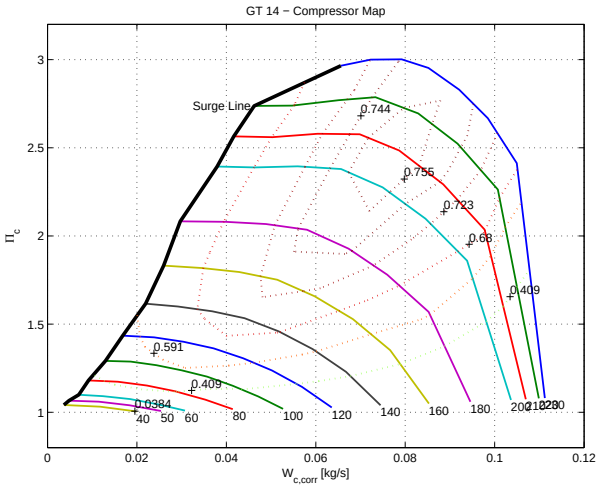

Fig. 3. Example of a compressor map for car engine applications. Pressure ratio is plotted against corrected mass flow for different speed lines (given in thousands of rpm).

incorporates an additional state for the mass flow. An example of a compressor map is shown in figure 3. The surge line is the points on each speed line with lowest flow. These endpoints were determined by the gas stand operator as the smallest mass flow that had a stable reading on the gas stand mass flow meter. In the model it is necessary to have a description of the speed lines. Here a simple parametrization is used. The compressor map is parametrized using the compressible dimensionless quantities for flow Φ and energy Ψ. They are defined as (Dixon, 1998)

$$\Phi = \frac{W_c}{ND^3}\frac{RT_{bc}}{p_{bc}} \tag{3}$$

$$\Psi = \frac{c_p T_{bc}(\Pi_c^{(\gamma-1)/\gamma} - 1)}{N^2 D^2} \tag{4}$$

where D is the compressor diameter, N is the rotational speed and R is the specific gas constant for air. When transformed into the $\Phi - \Psi$ domain, the speed lines in the compressor map gathers into almost a single curve (Eriksson, 2007). The model uses the relation between Φ and Ψ to span the compressor map and it is represented by the combination of a third and a second order polynomial (5).

$$\Psi(\Phi) = \begin{cases} a_3\Phi^3 + a_2\Phi^2 + a_1\Phi + a_0 & \text{if } \Phi \leq \Phi_{\Psi_{max}}, \\ b_2\Phi^2 + b_1\Phi + b_0 & \text{if } \Phi > \Phi_{\Psi_{max}} \end{cases} \tag{5}$$

The separation into two regions increases the flexibility when studying the effect of the compressor map on co-surge. The shape of the speed lines in the surge region can be varied without altering the nominal region in the map and vice versa. The parameters a_i and b_i in $\Psi(\Phi)$ are determined from the parameters Ψ_{max}, $\Delta\Psi$, $\Phi_{\Psi_{max}}$ and Φ_0 together with the constraints $\Psi'(0) = 0$ and $\Psi'(\Phi_{\Psi_{max}}) = 0$, see figure 4. The most interesting part of the compressor map for this investigation is the region closest to the surge line and pressure ratios around $\Pi = 1.5$. For the test vehicle this is a high load operating point where measurements on co-surge have been made, and thus the model parameters are tuned to give best accuracy in that region. Compressor maps do not normally cover the surge region. The $\Delta\Psi$ parameter, that determines

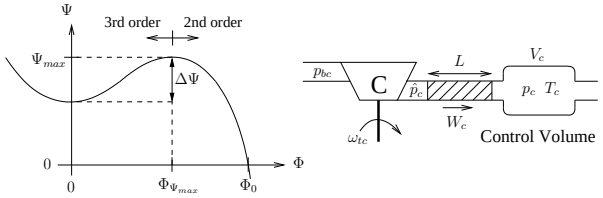

Fig. 4. *Left:* Parameterization of the $\Phi - \Psi$ function. *Right:* The More-Greitzer compressor model, the pressure difference $\hat{p}_c - p_c$ results in an acceleration of the flow plug that governs the mass flow.

the dip of the speed line in the surge region, has been matched to recent work on surge capable compressor models by Leufven and Eriksson (2010). The pressure build up, $\hat{p}_c$, is calculated from the current mass flow and speed by using equations (3) and (5) to find Ψ and solving (4) for the pressure after the compressor, giving

$$\hat{p}_c = \left(\frac{\Psi N^2 D^2}{c_p T_{bc}} + 1\right)^{\frac{\gamma}{\gamma-1}} p_{bc} \tag{6}$$

The difference between pressure build up, $\hat{p}_c$ and pressure after the compressor, p_c, results in a force that accelerates a flow plug that govern the mass flow.

$$\frac{dW_c}{dt} = \frac{\pi D^2}{4L}(\hat{p}_c - p_c) \tag{7}$$

4.1 Compressor efficiency

The temperature out of the compressor is determined by the compressor efficiency defined as

$$\eta_c = \frac{(\Pi_c)^{\frac{\gamma-1}{\gamma}} - 1}{\frac{T_{out}}{T_{in}} - 1} \tag{8}$$

Here it is important to note that during a surge cycle, the flow reverses and the compressor works as a turbine. The efficiency definition differs between compressor and turbine operation by the change of denominator and numerator in 8, and inversion of the pressure ratio. For the surge capable compressor the temperature of the flow are therefore determined by

$$T_{out} = T_{in}\left(1 - \frac{1}{\eta_c^{sgn(W_c)}}\left(1 - (\Pi_c^{sgn(W_c)})^{\frac{\gamma-1}{\gamma}}\right)\right) \tag{9}$$

The compressor efficiency η_c is modeled from the compressor map as a product of η_{max}, the maximum efficiency, η_Φ and η_N, suggested as one alternative in Eriksson (2007). The later two describe the efficiency decrease when Φ and N diverge from their value at the maximum efficiency point.

5. ANALYSIS OF SURGE PROPERTIES

The integrated engine and compressor models presented in sections 3 and 4 were used in simulation to re-create the measured co-surge cycles. A simulation is shown in figure 5. With parameters that correspond to the engine used in the measurements, the frequency in the co-surge oscillations is only slightly higher. The shape of the mass flow differs more. In the measured data the switch is simultaneous in the sense that one mass flow drops at the same time as one mass flow increases. In the simulation with this model one mass flow first recovers, then there

Table 1. Properties of the co-surge cycles for simulations with different parameter variations. Largest influence comes from $\Delta\Psi$, the compressor inertia and the volumes after the compressor. The phase deviation from 180° is small enough to be numerical errors.

Simulation	Frequency [Hz]		Δp [kPa]		Phase [deg]	
Standard	2.05	+0%	10.2	+0%	179	+0.0°
V_{af}x2	2.15	+5%	10.1	-1%	181	+1.3°
V_{af}x0.5	2.05	+0%	10.6	+4%	181	+1.2°
V_cx2	1.56	-24%	9.2	-10%	177	-2.5°
V_cx0.5	2.64	+29%	10.8	+7%	181	+1.3°
V_{ic}x2	1.66	-19%	9.6	-5%	177	-2.2°
V_{ic}x0.5	2.34	+14%	10.3	+2%	179	-0.7°
Lx2	2.05	+0%	10.4	+2%	179	-0.0°
Lx0.5	2.15	+5%	10.1	-0%	181	+1.8°
J_{tc}x2	1.76	-14%	11.8	+16%	178	-1.2°
J_{tc}x0.5	2.64	+29%	8.4	-17%	180	+0.5°
$\Delta\Psi$x1.5	1.46	-29%	14.8	+45%	179	-0.1°
$\Delta\Psi$x0.75	2.44	+19%	7.7	-24%	182	+2.3°

is a period of time before the other mass flow drops. The switch between forward an backward flow is also faster in the simulation, but this can partly be explained by the absence of sensor dynamics in the model. The amplitude of the pressure oscillation is 10 kPa in the simulation, 3 kPa larger than the measurements. This variation could be the result of a slightly too large Δ_Ψ parameter, which has a very large effect on the pressure amplitude.

To investigate the sensitivity to different parameter variations a simulation series was performed. The results are presented in table 1. The parameters that have the largest influence on the frequency are the dip in the Ψ-Φ function, $\Delta\Psi$, the turbocharger inertia, J_{tc} and the volumes after the compressor, V_c and V_{ic}. The pressure dip is mostly affected by $\Delta\Psi$. The phase is almost 180° in all simulations, the small spread can be explained by the oscillation being not completely stationary and inaccuracy in the computation. The frequencies in the simulations range between $1.5 - 2.5$ Hz which covers the frequency in the measurements. There are differences between the simulations and measurements and there will be variations in the model parameters through the use of lumped parameter models and uncertainty in the engine parameters, when tuning the model against data. This shows that the differences can be captured with small parameter variations, keeping the physical interpretation of the model.

6. PIPE DYNAMICS INVESTIGATION

Although the frequency and pressure oscillations of co-surge is captured by the MVEM and More-Greitzer compressor model, the shape of the mass flow does not fully resemble the measured data. The More-Greitzer model only includes momentum of a single flow plug after the compressor to model surge. Since the flow direction around the compressors switch back and forth during surge, the momentum of the gas in the pipes, both before and after the compressor, could have a large influence on the behavior. Therefore the effect of including a more detailed model of gas momentum in the pipes is investigated, by splitting the control volumes into several sections. Each section uses the equations for an ordinary control volume, but the mass

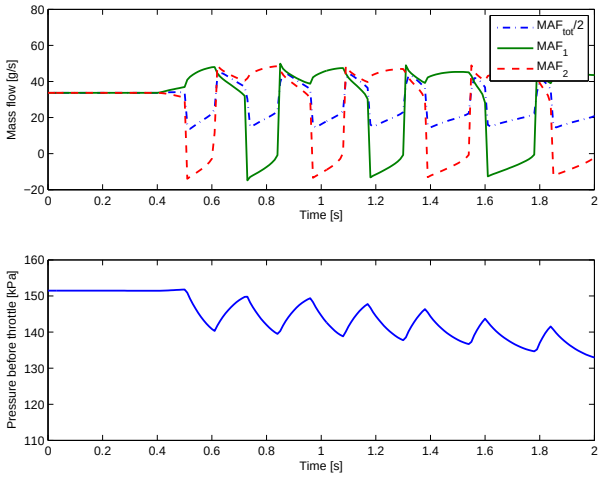

Fig. 5. Co-Surge simulation with the standard MVEM and More-Greizer compressor model. The oscillation has almost the same frequency as the measured data. The amplitude of the pressure oscillation is 10 kPa which slightly higher then in the measurements.

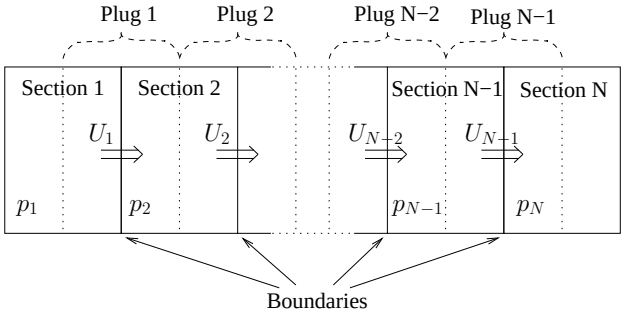

Fig. 6. Model of pipe with momentum conservation. The control volume is split into several sections with a flow plug that governs the mass flow across the boundaries.

flow across the boundary of each section is governed by a flow plug. The flow plug is considered to have a mass equal to half the mass of the sections upstream and downstream of the plug, see figure 6 for an illustration. The acceleration of the plug is then determined by Newton's law of motion

$$\frac{dU_i}{dt} = \frac{2A(p_i - p_{i+1})}{m_i - m_{i+1}} - U_i k_{fric} \tag{10}$$

where U_i is the velocity of plug i, and p_i and m_i are the pressure and mass in control volume i. The damping term k_i represents friction in the pipes. This model which is used in Öberg and Eriksson (2007); Öberg (2009) is a simplified model of Andersen et al. (2006). Exchanging the standard control volume before and after the compressor, the effect of momentum conservation in the control volumes has been investigated.

6.1 Simulations with pipe dynamics

One simulation with pipe dynamics added to the model is shown in figure 7. In this simulation the pipes with dynamics have ten sections each. The co-surge oscillation frequency decreases by roughly 25% compared to the model without pipe dynamics with the same parameters. The mass flow becomes more oscillatory and the spike in mass flow after the switch in the measured data can

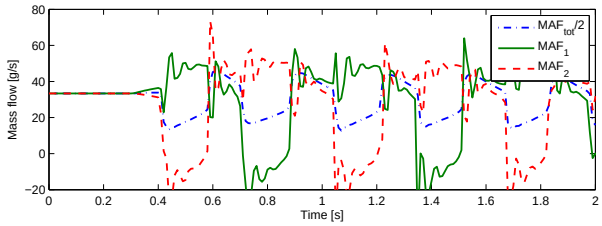

Fig. 7. Co-Surge in the simulation model with pipe dynamics before and after the compressor. The spike in mass flow after the switch from backward to forward seen in the measured data flow is now visible in the simulation, but the switch is still not simultaneous.

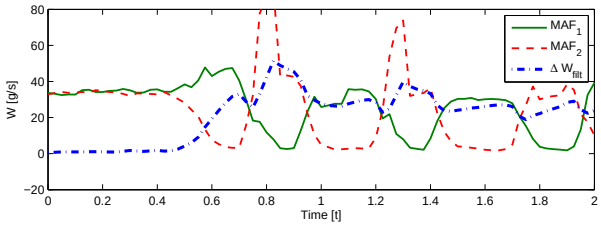

Fig. 8. The detection procedure evaluated on a co-surge measurement. The green solid and the red dashed lines are the two mass flows, and the blue dash-dotted line is the filtered mass flow difference. For a threshold of 10 g/s, detection of co-surge would occur 0.13 s after the mass flows diverge.

now be seen in the simulation. However, the switching between reverse and forward flow for the compressors is still not simultaneous. The sensitivity to parameter changes is similar to the model without pipe dynamics, but with the addition of pipe dynamics the influence of the control volume parameters is relatively larger. The main disadvantage of including pipe dynamics is that the model becomes more complex and stiff which increases simulation time. Since the qualitative properties are the same, the simpler model is considered to be enough for control purposes and is therefore used in the next section.

7. CONTROL

To have the largest margin to the surge line for both compressors in a given operating point, the control system should strive for balance between the two mass flows. If co-surge occurs, the control system should take measures to stabilize the flows i.e. to minimize $\Delta W = |W_1 - W_2|$. This section presents a control strategy for quelling the mass flow oscillations that utilizes the two mass flow sensors, MAF_1 and MAF_2, and use additive commands in the two surge valves and throttle, u_{sv1}, u_{sv2} and u_{thr}, see figure 2. The control strategy is evaluated on the developed engine model together with a detection algorithm that is the topic of the next subsection.

7.1 Detection

The detection algorithm is based on the difference in mass flow. The absolute value of this signal is filtered through a first order low pass filter with high cut-off frequency, removing disturbances while keeping a fast reaction time to unbalances. If the filtered signal is larger than the threshold value ΔW_{level}, co-surge is detected, see equation 11. The filter coefficient, k, and the threshold, ΔW_{level}, together determine the detection time and sensitivity to disturbances. Figure 8 shows how this works on one of the co-surge measurements. In this test case, a filter coefficient corresponding to 0.1 s rise time for the low-pass filter and a threshold of 10 g/s, would give detection 0.13 s after the mass flows diverge.

$$\frac{1-k}{1-kz^{-1}}|W_1 - W_2| >= \Delta W_{level} \implies CS_{detect} = 1 \quad (11)$$

7.2 Co-surge quelling

When co-surge occurs due to a disturbance between the two mass flows, pushing one compressor into reverse flow, the original operating point with balanced mass flow is stable. The objective is therefore to quell the oscillation and return to this operating point as fast as possible and with as little torque disturbance as possible. The fast actuators that quickly can change the compressor operating point are the throttle and the surge valves. Opening the throttle moves the surge line to the left in the compressor map. Opening the surge valve reduces the pressure ratio and increases the mass flow felt by the compressor by recirculating a part of the compressed air.

Opening the surge valve too much or for too long will cause a large drop in boost pressure and thus reduced torque, which is undesirable. On the other hand, opening the throttle might not be enough if the opening angle already is large, and if the mass flow recovers it will be in an operating point with higher mass flow producing excess torque. Combining the two gives fast recovery and small torque disturbance.

When co-surge is detected the throttle is opened up and a small surge valve opening is commanded. When the flows equilibrate the surge valve is immediately closed and the throttle valve ramped down to its previous value, according to:

$$u_{sv}^{+} = k_{sv} CS_{detect} \quad (12a)$$

$$u_{thr}^{+} = \begin{cases} k_{thr} & \text{if } CS_{detect} = 1 \\ u_{thr}^{+}(k-1) - k_{thr}\dfrac{\tau_s}{\tau_{thr}} & \text{if } CS_{detect} = 0 \end{cases} \quad (12b)$$

Where u_{sv}^{+} and u_{thr}^{+} are additive to the surge valve and throttle command, $u_{thr}^{+}(k-1)$ indicates the previous sample, τ_s is the sample time and τ_{thr} is a tuning parameter that determines how fast the throttle is ramped down. The other tuning parameters are k_{sv} and k_{thr} that determine the size of the additive commands. They need to be large enough to quickly get out of surge but as small as possible to reduce torque disturbance. Future work is to develop a systematic method for the parameter tuning.

In figure 9 the control action is shown where the complete MVEM is used. A disturbance in the mass flow balance has been induced at time zero, pushing one flow into reverse. When one mass flow reverses the pressure and torque drops. As co-surge is detected at 0.05 s, the throttle and surge valve opens up and the reverse mass flow quickly recovers. When the co-surge indication drops, the surge valve is closed and the throttle is ramped down.

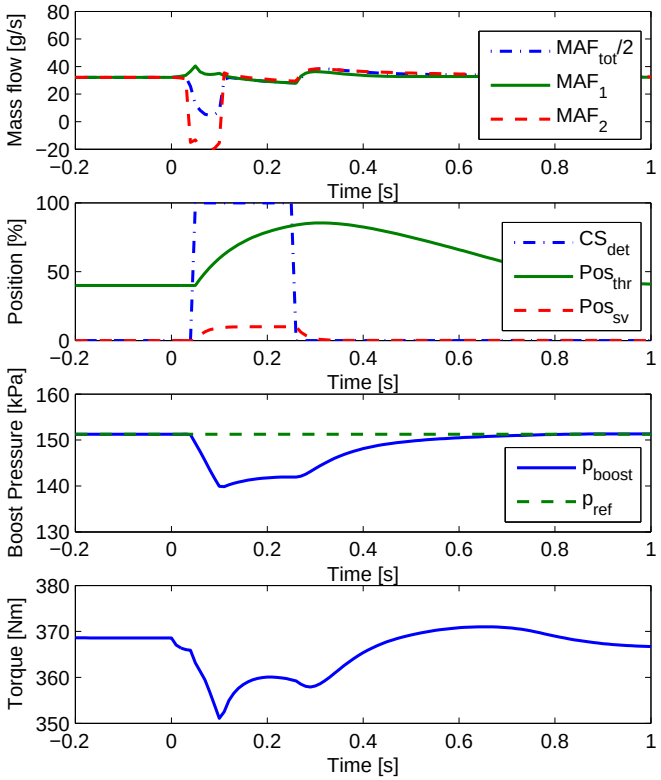

Fig. 9. The described stabilization method evaluated on the model. The engine is operating in a stable operating point close to the surge line. At time zero a disturbance alters the mass flow balance, pushing one flow into reverse. When this is detected, the throttle is opened up together with a small and short opening of the surge valves. A stable operation is recovered and the torque is back to level within 0.5 s

Within 0.5 s the mass flows are balanced and the torque has reached the level before the disturbance.

8. CONCLUSIONS

Co-Surge in bi-turbocharged engines is analyzed. Measurements are presented where co-surge frequency is an order of magnitude lower than standard compressor surge, indicating that co-surge is more than standard compressor surge with alternating flow reversals. A model of a bi-turbocharged engine that can capture the frequency and amplitude of the co-surge phenomenon has been developed. In a validation against measured data it is shown that a mean value engine model together with a More-Greizer compressor model can capture the co-surge frequency but not fully recreate the shape of the mass flow oscillation. With the addition of momentum conservation in the pipes the agreement with measurement can be slightly improved, at the price of increased simulation time. A detection algorithm and a control strategy to quell co-surge is presented. The detection algorithm is shown to quickly detect co-surge in the measured data. Simulations on the model show that when the control is switched on, mass flow balance and torque level are recovered in 0.5 s.

REFERENCES

Ammann, M., Fekete, N.P., Amstutz, A., and Guzzella, L. (2001). Control-oriented modeling of a turbocharged common-rail diesel engine. In *Proceedings from the 3rd. Int. Conference on Control and Diagnostics in Automotive Applications (CD Auto ´01), Sestri Levante.*

Andersen, S.K., Carlsen, H., and Thomsen, P.G. (2006). Control volume based modelling in one space dimension of oscillating, compressible flow in reciprocating machines. *Simulation Modelling Practice and Theory*, 14, 1073–1086.

Andersson, P. (2005). *Air Charge Estimation in Turbocharged Spark Ignition Engines.* Ph.D. thesis, Linköping University.

Dixon, S. (1998). *Fluid Mechanics and Thermodynamics of Turbomachinery.* Butterworth-Heinemann, 4th edition.

Eriksson, L. (2007). Modeling and control of turbocharged SI and DI engines. *Oil & Gas Science and Technology - Rev. IFP*, 62(4), 523–538.

Eriksson, L., Nielsen, L., Brugård, J., Bergström, J., Pettersson, F., and Andersson, P. (2002). Modeling of a turbocharged SI engine. *Annual Reviews in Control*, 26(1), 129–137.

Gravdahl, J.T. (1998). *Modeling and Control of Surge and Rotating Stall in Compressors.* Ph.D. thesis, Norweigan University of Science and Technology.

Greitzer, E. (1981). The stability of pumping systems. *Journal of Fluids Engineering, Transactions of the ASME*, 103(1), 193–242.

Leufven, O. and Eriksson, L. (2008). Time to surge concept and surge control for acceleration performance. IFAC World Congress. Seoul, Korea.

Leufven, O. and Eriksson, L. (2010). Surge and choke capable compressor model. IFAC World Congress 2011.

Öberg, P. (2009). *A DAE Formulation for Multi-Zone Thermodynamic Models and its Application to CVCP Engines.* Ph.D. thesis, Linköping University.

Öberg, P. and Eriksson, L. (2007). Control oriented gas exchange models for CVCP engines and their transient sensitivity. *Oil & Gas Science and Technology - Rev. IFP*, 62(4), 573–584.

Willems, F. and de Jager, B. (1998). Modeling and control of rotating stall and surge: An overview. In *Int. Conference on Control Applications*, 331–335.

Appendix A. NOMENCLATURE

Symbol	Description	Subscript	Description
c_p	Specific heat	*af*	Air filter
γ	c_p/c_v	*bc*	Before compressor
η	Efficiency	*c*	Compressor
J	Inertia	*fric*	Friction
L	flow plug length	*ic*	Intercooler
MAF	Mass flow sensor	*im*	Intake manifold
N	Rotation speed	*t*	Turbine
Π	Pressure ratio	*tc*	Turbocharger
P	Power	*thr*	Throttle
p	Pressure	*sv*	Surge valve
R	Gas constant		
T	Temperature		
u	Control signal		
V	Volume		
W	Mass flow		
ω	Angular velocity		